Journal of Applied Mechanics and Technical Physics, Vol. 38, No. 1, 1997

AN EXPERIMENTAL STUDY OF GENERATION OF UNSTABLE DISTURBANCES ON THE LEADING EDGE OF A PLATE AT M = 2

A. D. Kosinov, A. A. Maslov, and N. V. Semionov

UDC 532.526

It is universally accepted that the laminar-turbulent transition in a boundary layer is related to instability (amplification of disturbances which induce the transition) and receptivity. Receptivity is usually understood as a mechanism whereby various external disturbances generate unstable oscillations of a boundary layer, thus leading to transition [1].

The majority of theoretical and experimental studies on receptivity were carried out for subsonic flows [2–4]. These studies have shown that external perturbations become eigenwaves of a boundary layer at the leading edge of the model and on the flow inhomogeneities caused by roughnesses, local separations, etc. [2–7].

The first attempt at theoretical investigation of the interaction of acoustic waves and a supersonic boundary layer using the theory of stability was undertaken by Mack [8]. He found that under the influence of sound, oscillations whose amplitude exceeds that of acoustic waves by severalfold arise in the boundary layer. Similar studies were carried out by Gaponov [9]. Some recent theoretical papers deal with the role of the leading edge in the receptivity of the supersonic boundary layer to external acoustic waves [10–12]. Fedorov and Khokhlov [11] analyzed the excitation of the first and second modes of the boundary layer near a sharp leading edge of a plate by longitudinal acoustic waves. This excitation is caused by the sound diffraction induced by the displacement effect of the boundary layer. The results of [11] are extended in [12] to the case of an arbitrary incidence angle of an external wave; two excitation mechanisms are identified: one of these is related to sound diffraction, and the other is connected with the occurrence of sources of an acoustic field when the wave is scattered on the leading edge. The generation of unstable waves in the boundary layer was found to depend on the acoustic-wave angle and on whether the sound source is located above or below. The excitation of the boundary-layer oscillations by a longitudinal acoustic field was studied by Gaponov [13], and a strong dependence of intensity of disturbances inside the layer on the spatial orientation of the external acoustic wave was obtained. Note that the conclusions of [12, 13] need experimental verification.

The first experiments on the laminar-turbulent transition were concerned with studying the influence of external factors (free-stream turbulence level, vibration of the model, and acoustic background) on the transition. A full description of these experiments is presented in [14]. However, to understand the transition process, one should first study the origin and development of unstable waves which induce the transition. Such an approach for the Mach number M = 1.6–8.5 was used by Kendall [15], who studied the development of natural disturbances in the boundary layer, and measured the correlation factor between the free-stream and boundary-layer oscillations. A high intensity of disturbances was found to be caused by an external acoustic field in the boundary layer close to the leading edge. A substantial effect of aerodynamic noise on the boundary layer also led to a monotonic growth of disturbances immediately at the leading edge of the model at M > 3. Correlation measurements showed that the correlation factors increase with an increase in M. Comparison of the experimental data of [15] with the numerical results of Mack's stability theory [16] showed good agreement for M = 4.5, while for M = 2.2, the measured growth rates differed from the calculated rates nearly by a factor of two. Since the experiments of [15] were performed for natural disturbances, the growth rates obtained were indicative only of the mean amplification of waves in the boundary layer. A correct comparison of the

Institute of Theoretical and Applied Mechanics, Siberian Division, Russian Academy of Sciences, Novosibirsk 630090. Translated from Prikladnaya Mekhanika i Tekhnicheskaya Fizika, Vol. 38, No. 1, pp. 51–57, January–February, 1997. Original article submitted September 25, 1995.

0021-8944/97/3801-0045 $18.00

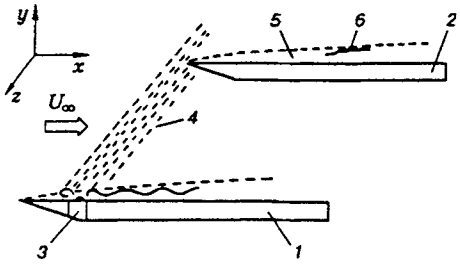

Fig. 1

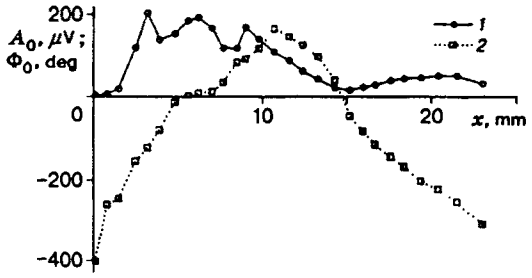

Fig. 2

theoretical and experimental results requires information on the wave angle, which is rather problematic for the case of natural disturbances.

The use of controlled disturbances in an experiment helps to get a correct comparison in studies of the origin of turbulence [17, 18]. The development of a source of controlled disturbances at supersonic speeds [19] also allowed an experimental study of receptivity to be performed [20–22]. Maslov and Semionov [21] found that the most intense generation of eigenoscillations of the supersonic boundary layer by acoustic waves occurs at the leading edge of the model, on the lower branch of the neutral-stability curve, and on the "sonic" branch of neutral stability. Kosinov et al. [22] studied the structure of boundary-layer disturbances that were generated by sound upon incidence of maximum radiation on the leading edge of the plate, and he compared this structure with the structure of disturbances generated by a point source in the boundary layer. The results of [20–22] showed a complex picture of transformation of acoustic waves into unstable disturbances of the supersonic boundary layer.

Experiments on the generation of unstable disturbances in the supersonic boundary layer on the leading edge of a plate by external controlled disturbances are reported in the present paper. The wave spectra of initial disturbances and the boundary-layer disturbances generated by them are determined.

The experiments were carried out in the T-325 supersonic wind tunnel of the Institute of Theoretical and Applied Mechanics of the Siberian Division of the Russian Academy of Sciences with a $200 \times 200 \times 600$ mm test section at a Mach number M = 2 and a unit Reynolds number $\mathrm{Re}_1 = 6.6 \cdot 10^6$ 1/m. A diagram of the experiment model is shown in Fig. 1 (1 and 2 are the plates, 3 is the generator of periodic disturbances, 4 is the controlled disturbances, 5 is the boundary layer, and 6 is the hot-wire probe). Plate 1 with the generator of periodic disturbances was mounted on the rod of a traversing gear and could be moved in the normal direction. The disturbances were sufficiently strong to radiate acoustic waves into the free stream [23]. They were generated by a high-frequency electric discharge with frequency $f = 20$ kHz [the dimensionless frequency parameter was $F = 2\pi f/(\mathrm{Re}_1 U) = 0.38 \cdot 10^{-4}$, where U is the free-stream velocity]. The design of the source of disturbances and the scheme of measurements were the same as in [24].

The source of controlled disturbances can be positioned either above or below the model. In the experiments of [21], a plate with a discharge was above the model. Although the maximum of radiation is incident on the leading edge of the plate in this case, the external acoustic field also generated boundary-layer disturbances in other regions, and this made data processing more difficult. Therefore, the experimental layout was such that the source of acoustic waves was located below the plate (Fig. 1); then the disturbances in the boundary layer were generated only near the leading edge of the plate. A constant-temperature hot-wire anemometer and a single-wire probe with a tungsten wire 5 μm in diameter and 1.2 mm long were used for disturbance measurements. The probe moved along the x and z coordinates with a step of 0.1 mm and along the y coordinate with a step of 0.01 mm. The pulsation signal from the hot-wire anemometer was sent to a computer through an ADC. Simultaneous summation of the signal from 200 points was performed directly during the experiment to increase the signal-to-noise ratio. The measurements in the boundary layer were performed for $y/\delta = \mathrm{const}$, in the layer with maximum oscillations (δ is the boundary-layer thickness).

To find the generation coefficients of unstable waves, we measured the initial distributions of the amplitude $A_0(f,x,z)$ and the phase $\Phi_0(f,x,z)$ of acoustic waves near the leading edge of the model and the field of disturbances $A(f,x,z)$ and $\Phi(f,x,z)$ inside the boundary layer of plate 2. Discrete Fourier transform [17] was used to determine the spectra from the wavenumbers. The results of data processing were presented as the amplitude $A_f(\chi)$ and the phase $\Phi_f(\chi)$ of disturbances for $f = \text{const}$ versus the wave angle to the flow $\chi = \arctan(\beta/\alpha_r)$ (α_r and β are the wavenumbers in the x and z directions, respectively). The values of α_r and β were found from the relation

$$A_f(\alpha_r,\beta)\exp(i\Phi_f(\alpha_r,\beta)) = 1/T\sum E(x_i,z_j,t_k)\exp(-i(\alpha_r x_i + \beta z_j - 2\pi f t_k)),$$

where $E(x_i,z_j,t_k)$ is the discrete signal from the hot-wire probe averaged over realizations and T is the time of realization. The transfer functions of disturbances (the generation coefficient) were found from the relation $K(\chi) = A_f(\chi)\big|_{x=x_i} \big/ A_f(\chi)\big|_{x=x_0}$ (the ratio of the amplitude of disturbances generated in the boundary layer to the amplitude of acoustic waves incident on the leading edge).

The initial conditions were found by measuring the field of controlled disturbances in the free stream in the plane of plate 2 (the plate was removed). Figure 2 shows the amplitude $A_0(x)$ and the phase $\Phi_0(x)$ (curves 1 and 2, respectively) as functions of the longitudinal x coordinate in the plane of plate 2 for $z = 0$. The x coordinate was measured downstream of the boundary of radiation.

For analysis of the data obtained, it is useful to imagine a simplified physical model of the source of disturbances. The discharge being initiated, the electric arc extends over the plate surface. Deceleration of the flow in the near field upstream and downstream of the discharge possibly results in the formation of vortices with different directions of rotation in the plane yx. Further downstream, the generated disturbances lead to the formation of Tollmien–Schlichting (TSh) waves in the boundary layer of plate 1. This process is accompanied by the radiation of various types of controlled disturbances into the free stream. The radiation propagates inside the Mach cone from the discharge. Using this model and the functions $A_0(x)$ and $\Phi_0(x)$, we distinguished typical regions that correspond to various types of controlled disturbances. The radiation from the vortex upstream of the discharge corresponds to the region of approximately $1.5\,\text{mm} < x < 5$ mm, the radiation behind the discharge corresponds to $9\,\text{mm} < x < 13$ mm, and the radiation from the TSh waves to $14\text{ mm} < x$.

Figure 3 shows the amplitude spectrum of radiation A_0 versus the wavenumber α_r in the x direction obtained by processing the data of Fig. 2. Here the amplitude is normalized to its maximum. The distribution $A_0(\alpha_r)$ has two maxima: $\alpha_r = -0.45$ and $\alpha_r = 0.75$ rad/mm. The first maximum corresponds to the vortex radiation upstream of the discharge, and the second corresponds to the radiation from the other zones. This correspondence between the maxima in the distribution $A_f(\alpha_r)$ and the radiation zones becomes evident if the experimental $A_0(x)$ and $\Phi_0(x)$ are treated separately for the regions $1.5\,\text{mm} < x < 7$ mm and $9\,\text{mm} < x < 23$ mm. From the values of α_r, the phase velocity of controlled disturbances in the x direction, $C = 2\pi f/(\alpha_r U)$, was obtained. For the first region of radiation, $C = -0.54$. The negative value of C corresponds to upstream propagating disturbances. For the second and third radiation regions, $C = 0.33$, which corresponds to acoustic disturbances.

For cross sections $x = \text{const}$ in three different regions of radiation ($x = 3.5$, 11, and 23 mm), the distributions $A(z)$ and $\Phi(z)$ were measured, and the spectra were determined from the wavenumber β.

In the study of the field of disturbances generated by external controlled waves inside the boundary layer, plate 2 was mounted so that its leading edge was sequentially positioned in those sections at which the external disturbances belonging to different regions of radiation were studied (i.e., the leading-edge coordinate was $x = 3.5$, 11, and 23 mm). The distributions $A(z)$ and $\Phi(z)$ were measured for two cross sections in the boundary layer of plate 2 ($x^* = 40$ and 50 mm, where x^* is the distance from the leading edge). The stable region of development of disturbances in the supersonic boundary layer was studied. The spectra were determined from the wavenumber β using these data and the discrete Fourier transform.

The amplitude and phase spectra of external acoustic disturbances and the eigenoscillations generated

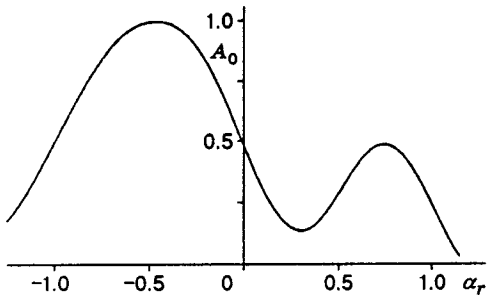

Fig. 3

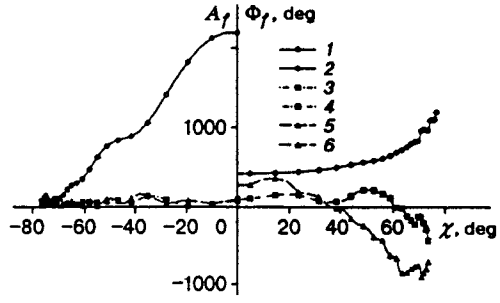

Fig. 4

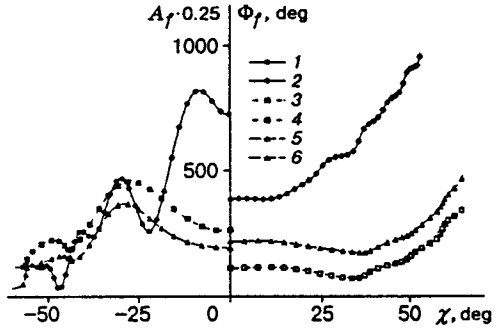

Fig. 5

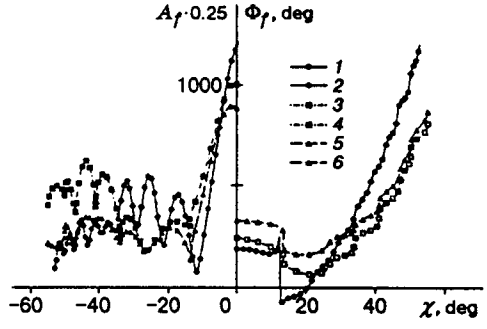

Fig. 6

by the disturbances are compared in Fig. 4 as functions of the wave angle χ for the leading-edge coordinate $x = 3.5$ mm. Curves 1 and 2 are the distributions $A_f(\chi)$ and $\Phi_f(\chi)$ of acoustic disturbances hitting the leading edge of the model, curves 3 and 4 are the distributions $A_f(\chi)$ and $\Phi_f(\chi)$ for the cross section in the boundary layer $x^* = 40$, and curves 5 and 6 show the same for $x^* = 50$ mm. One can see that the amplitude of eigenoscillations in the boundary layer is close to zero and comparable with the noise. Although the distribution $\Phi_f(\chi)$ for the boundary-layer oscillations shows that the generation by external controlled disturbances does occur, the transfer function is close to zero. Thus, upstream-propagating, external disturbances practically do not bring about a response in the supersonic boundary layer.

A different picture is observed for the radiation from downstream-propagating disturbances. In this case, disturbances are excited in the boundary layer, and the amplitudes of acoustic radiation and forced disturbances can be compared.

Figure 5 shows the distributions $A_f(\chi)$ and $\Phi_f(\chi)$ of external acoustic disturbances and oscillations generated by them for $x = 11$ mm. The notation is the same as in Fig. 4. Note that the distributions $A_f(\beta)$ and $\Phi_f(\beta)$ in the external flow and in the boundary layer are similar [17], but the difference in the phase velocities C between the acoustic disturbances and the boundary-layer oscillations leads to a difference in the angles χ. The amplitude of oblique waves with $\chi \approx 10$ and 30° is maximal in the vortex radiation immediately behind the discharge, and disturbances with $\chi \approx 30°$ are generated in the boundary layer.

Figure 6 shows the distributions $A_f(\chi)$ and $\Phi_f(\chi)$ of external acoustic disturbances and the oscillations generated by them for $x = 23$ mm (the notation is the same as in Fig. 4). The distributions $A_f(\chi)$ and $\Phi_f(\chi)$ in the external flow and in the boundary layer are similar. The main maximum of $A(\chi)$ is observed for $\chi = 0$, and this is in good agreement with the results of [23], where the radiation from TSh waves was studied. The oblique waves have a much smaller amplitude, but the oscillations in the boundary layer exceed the external acoustic disturbances even for $\chi \geqslant 35°$. Note that the experimental distributions $A(z)$ and $\Phi(z)$ agree qualitatively with the data of [22], where the structure of the boundary-layer disturbances generated

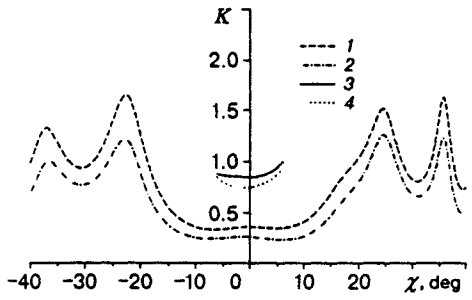

Fig. 7

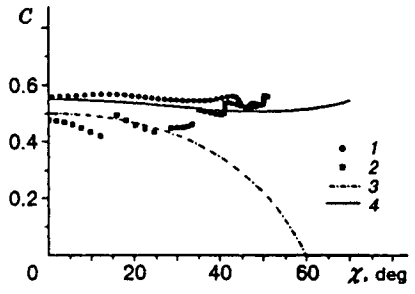

Fig. 8

by sound incident on the leading edge from above was studied. Modulation in $A(x, z)$ was observed in both cases, and this indicates the existence of several types of disturbances in the boundary layer.

Figure 7 shows the transfer functions $K(\chi)$ of the disturbances excited by the second region of radiation. Confining ourselves to the lower level of the generated amplitude of disturbances close to $(1/3)A_{\max}$, we present the data within the range of angles $\chi \pm 40°$ for two values of the x^* coordinate (curves 1 and 2 for $x^* = 40$ and 50 mm). Two typical regions in which disturbances were generated were found, namely, the region of $\pm 10°$ with minimum generation coefficients and the region of $\pm(20°–40°)$ with maximum generation coefficients. Figure 7 also shows the results on disturbance generation for the third region of radiation (curves 3 and 4 for $x^* = 40$ and 50 mm). Imposing the same constraint on the level of amplitude, we present only the data for angles $\pm 6°$. There is a difference in the generation coefficients K for comparable wave angles for different regions of radiation. This difference can be caused by the fact that acoustic waves can be of a different nature: the radiation in the second region is generated by a stationary source, whereas the radiation in the third region is produced by moving vortices. The difference in the value of the coefficient K is explained by the possible difference in direction of acoustic radiation, which agrees with the conclusions of [12, 13], where a strong dependence of the intensity of disturbances inside the layer on the spatial orientation of the external acoustic wave was obtained.

One can see from Fig. 6 that the amplitude of the disturbances generated in the boundary layer with $\chi \geqslant 35°$ is higher than that of external acoustic disturbances, i.e., the generation coefficient $K > 1$. Hence, oblique waves are generated more intensely than a planar wave with $\chi \approx 0$. This result is in agreement with the theoretical result of [13].

Figure 8 shows the phase velocities of the boundary-layer perturbations generated by acoustic disturbances (points 1 and 2 are the phase velocities of the disturbances excited by the second and third regions of radiation, curve 3 is the critical phase velocities $C^* = 1 - 1/(\mathrm{M}\cos\chi)$ that separate waves with discrete and continuous spectra, and curve 4 shows the phase velocities of waves with discrete spectrum calculated by numerical integration of the Dan–Lin system for parameters that are close to the experimental parameters ($f = 20$ kHz and $\mathrm{Re} = 565$).

Note that the experimentally obtained phase velocities of the waves generated in the boundary layer in the second region of radiation are close to the theoretical values for TSh waves. Therefore, we shall class the results for the second region of radiation among waves of this type. The experimentally obtained phase velocities of the waves generated in the boundary layer in the third region of radiation were found to be smaller than those of TSh waves. This means that the waves generated in the boundary layer consist of different types of disturbances, for example, vortical and acoustic [17, 22, 23]. To separate these disturbances, one should study a larger number of x sections. Thus, when the radiation from the second region is incident on the leading edge of the model, TSh waves are excited in the boundary layer; the incidence of radiation from the third region generates both TSh waves and acoustic oscillations. Apparently, in these cases, there are different mechanisms of generation of boundary-layer disturbances in the vicinity of the leading edge of the model [12, 13], and this is caused by the different structure of radiation from different regions.

The authors are thankful to A. V. Fedorov for his suggestion in the formulation of the problem and to S. A. Gaponov for valuable discussions.

This work was supported by NASA (cooperation agreement NCCW-74).

REFERENCES

1. M. V. Morkovin, "On transition experiments at moderate supersonic speeds," *J. Aeronaut. Sci.*, **24**, No. 7, 480–486 (1957).
2. M. Nishioka and M. V. Morkovin, "Boundary-layer receptivity to unsteady pressure gradients: experiments and overview," *J. Fluid Mech.*, **171**, 219–262 (1986).
3. Y. S. Kachanov, V. V. Kozlov, and V. Ya. Levchenko, *Occurrence of Turbulence in Boundary Layers* [in Russian], Nauka, Novosibirsk (1981).
4. M. E. Goldstein and L. S. Hultgren, "Boundary-layer receptivity to long-wave free-stream disturbances," *Ann. Rev. Fluid Mech.*, **21**, 137–166 (1989).
5. M. E. Goldstein, "The evolution of Tollmien–Schlichting waves near a leading edge," *J. Fluid Mech.*, **127**, 59–81 (1983).
6. M. Choudhari and C. L. Street, "A finite Reynolds-number approach for the prediction of boundary-layer receptivity in localized regions," *Phys. Fluids A*, **4**, No. 11, 2495–2514 (1992).
7. L. B. Aizin and N. F. Polyakov, "Generation of Tollmien–Schlichting waves by sound on an isolated roughness of the surface in flow," Preprint No. 17, Inst. Theor. Appl. Mech., Sib. Div., USSR Acad. Sci., Novosibirsk (1979).
8. L. M. Mack, "Linear stability theory and the problem of supersonic boundary layer transition," *AIAA J.*, **13**, 423–448 (1975).
9. S. A. Gaponov, "Interaction of a supersonic boundary layer with acoustic disturbances," *Izv. Akad. Nauk SSSR, Mekh. Zhidk. Gaza*, No. 6, 51–56 (1977).
10. P. W. Duck, "The response of a laminar boundary layer in supersonic flow to small amplitude progressive waves," *J. Fluid Mech.*, **219**, 423–448 (1990).
11. A. V. Fedorov and A. P. Khokhlov, "Excitation of unstable modes by acoustic waves in a supersonic boundary layer," *Izv. Akad. Nauk SSSR, Mekh. Zhidk. Gaza*, No. 4, 67–74 (1991).
12. A. V. Fedorov and A. P. Khokhlov, "Receptivity of a supersonic boundary layer to acoustic disturbances," *Izv. Akad. Nauk SSSR, Mekh. Zhidk. Gaza*, No. 1, 40–47 (1992).
13. S. A. Gaponov, "On the interaction of a supersonic boundary layer with acoustic waves," *Teplofiz. Aeromekh.*, **2**, No. 3, 209–217 (1995).
14. S. A. Gaponov and A. A. Maslov, *Development of Disturbances in Compressible Flows* [in Russian], Nauka, Novosibirsk (1980).
15. J. M. Kendall, "Wind tunnel experiments relating to supersonic and hypersonic boundary-layer transition," *AIAA J.*, **13**, No. 3, 290–299 (1975).
16. L. M. Mack, "Boundary layer stability theory," Document 900-277, Pasadena, California–JPL (1969).
17. A. D. Kosinov, A. A. Maslov, and S. G. Shevel'kov, "Experiments on the stability of a supersonic laminar boundary layer," *J. Fluid Mech.*, **219**, 621–633 (1990).
18. P. Balakumar and M. R. Malik, "Discrete models and continuous spectra in supersonic boundary layers," *J. Fluid Mech.*, **239**, 631–656 (1992).
19. A. D. Kosinov, A. A. Maslov, and N. V. Semionov, "Methods for introducing artificial disturbances in a supersonic flow," Preprint No. 34-83, Inst. Theor. Appl. Mech., Sib. Div., USSR Acad. Sci., Novosibirsk (1983).
20. A. A. Maslov and N. V. Semionov, "Acoustic disturbances and supersonic boundary layers," in: *Problems on Nonlinear Acoustics*, Novosibirsk (1987), pp. 132–134.
21. A. A. Maslov and N. V. Semionov, "Excitation of natural oscillations of a boundary layer by an external acoustic field," *Izv. Akad. Nauk SSSR, Mekh. Zhidk. Gaza*, No. 3, 74–78 (1986).

22. A. D. Kosinov, A. A. Maslov, N. V. Semionov, and S. G. Shevel'kov, "Wave structure of artificial disturbances in a supersonic boundary layer on a plate," *Prikl. Mekh. Tekh. Fiz.*, No. 2, 95–98 (1990).
23. A. A. Maslov and N. V. Semionov, "Radiation of acoustic oscillations by a supersonic boundary layer," *Izv. Akad. Nauk SSSR, Ser. Tekh. Nauk*, **7**, No. 2, 58–63 (1987).
24. A. D. Kosinov, A. A. Maslov, and N. V. Semionov, "Methods of controlled disturbance generation for experimental investigation of supersonic boundary-layer receptivity," in: *Proc. Int. Conf. on Methods of Aerophysical Research* [in Russian], Novosibirsk (1994), pp. 138–144.